Tuning the wavelength of spoof plasmons by adjusting the impedance contrast in an array of penetrable inclusions

M.L. Cordero[1], A. Maurel[2], J.-F. Mercier[3], S. Félix[4] and F. Barra[1]
[1] *Departamento de Física Facultad de Ciencias Físicas y Matemáticas, Universidad de Chile Av. Blanco Encalada 2008 Santiago, Chile,*
[2] *Institut Langevin, CNRS, ESPCI ParisTech, 1 rue Jussieu, 75005 Paris, France,*
[3] *Poems, CNRS, ENSTA ParisTech, INRIA, 828 boulevard des Maréchaux 91762 Palaiseau, France,*
[4] *LAUM, CNRS, Université du Maine, avenue Olivier Messiaen, 72085 Le Mans, France.*

While spoof plasmons have been proposed in periodic arrays of sound-hard inclusions, we show that they also exist when inclusions are penetrable. Moreover, we show that their wavelength can be tuned by the impedance mismatch between the inclusion material and the surrounding medium, beyond the usual effect of filling fraction in the array. It is demonstrated that sound-soft materials increase the efficiency in the generation of sub-wavelength plasmons, with much lower wavelengths than sound-hard materials and than a homogeneous slab. An application to the generation of acoustic spoof plasmons by an ultra compact array of air/PDMS inclusions in water is proposed, with plasmon wavelength tunable up to deep sub-wavelength scales.

The notion of spoof plasmons has been introduced by Pendry and co-workers in the context of electromagnetic waves propagating in structured surfaces [1, 2] (see also Ref. [3] in the context of acoustics) as an alternative to the original surface plasmons, which require negative permittivity. In acoustics, surface plasmons are not easy to produce since this requires negative mass density, which is not available for natural materials. Acoustic spoof plasmons to the opposite can be produced, and their study has been limited to the case of arrays or gratings made of sound-hard materials [4, 5]. This is because most natural materials are stiff with respect to air or to water, resulting in large impedance mismatches. In the context of applied mathematics, spoof plasmons are called guided waves, existing in arrays of scatterers associated to the Neumann boundary condition [6]. These waves are inherently limited to $\lambda_{\rm SP}/\lambda > d/\ell$ (with ℓ the array width, d the array period, and $\lambda_{\rm SP}$ and λ the wavelengths of the plasmon and of the incident wave), which requires long inclusions, or wires, to reach low values of $\lambda_{\rm SP}$ [7]. On the other hand, guided waves by a homogeneous slab are known to exist and it is a limiting case of a structured array for a material filling fraction φ equal to unity. In this case, the resulting "plasmon" wavelength is given by the contrast in the sound velocity $\lambda_{\rm SP}/\lambda > c_1/c_0$ for sound velocity of the material, c_1, lower than the one of the surrounding medium, c_0.

With the development of man-made materials, it is now possible to design materials with independent control of the mass density and of the bulk modulus [8–10], including ultralight and ultrastiff materials [11]. In this paper, we consider an array of sound-penetrable inclusions and we show that the wavelength of the plasmons can be tuned by the mismatch of bulk modulus between the inclusions, B_1, and the surrounding medium, B_0. Indeed, the plasmon has a wavelength which scales typically as $\lambda_{\rm SP}/\lambda = \sqrt{\rho_1/\rho_0}\; c_1/c_0 = \sqrt{B_1/B_0}$, where ρ_0 and ρ_1 are the densities of the surrounding medium and of the inclusions, resulting in possibly very small plasmon wavelength. It is useful to note that the limit of unit filling fraction, $\varphi \to 1$, corresponding to a layer of sound soft material, is singular, and this will be described.

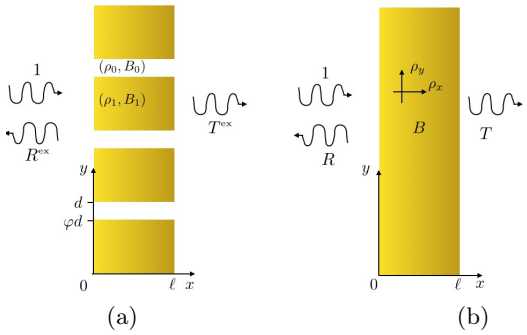

FIG. 1: (a) Geometry of the array. (b) Equivalent birefringent layer.

To begin with, we consider the wave equation,

$$\nabla \cdot \left(\frac{1}{\rho(x,y)} \nabla p(x,y) \right) + \frac{\omega^2}{B(x,y)}\, p(x,y) = 0, \qquad (1)$$

in the geometry depicted in Fig. 1, with $k = \omega\sqrt{\rho_0/B_0}$ the wavenumber in the surrounding medium and $k_1 = \omega\sqrt{\rho_1/B_1}$ in the inclusions, ω being the wave frequency. We define the ratio of the sound velocities and of the acoustic impedances

$$\begin{cases} \alpha \equiv \dfrac{c_0}{c_1}, \\ q \equiv \dfrac{\rho_0 c_0}{\rho_1 c_1}, \end{cases} \qquad (2)$$

between the inclusions and the surrounding medium.

For layered media, homogenization theory predicts an equivalence with a homogeneous but anisotropic medium, with an effective bulk modulus B and a density tensor, defined by its principal densities ρ_x and ρ_y [12]. Homogenization leads to

$$\nabla \cdot \left[\begin{pmatrix} 1/\rho_x & 0 \\ 0 & 1/\rho_y \end{pmatrix} \nabla p \right] + \frac{\omega^2}{B} p = 0, \tag{3}$$

with

$$\begin{cases} \dfrac{\rho_0}{\rho_x} = \varphi \dfrac{q}{\alpha} + 1 - \varphi, \\ \dfrac{\rho_y}{\rho_0} = \varphi \dfrac{\alpha}{q} + 1 - \varphi, \\ \dfrac{B_0}{B} = \varphi \alpha q + 1 - \varphi. \end{cases} \tag{4}$$

Note that, in this classical homogenization, the homogenized parameters depend only on the properties of the microstructure (material and geometry) because they are obtained from a static cell problem. In previous studies, non classical homogenizations, or effective medium theories, are based on approximated modal methods [2, 3, 13]. This can lead to effective parameters being frequency dependent.

Classical homogenization assumes that the typical size of the microstructure (say, the spacing d) is much smaller than the wavelength. Notably, this means that any resonances occurring within the unit cell is disregarded. Such resonances may appear if $kd > 1$ and this is the usual limitation of the homogenization process. For a penetrable array, the wavenumber inside the inclusions is $k_1 = \alpha k$ and resonances may also occur for $k_1 d$ values larger than unity. This is a well known problem of double limit in the homogenization theory, mainly in electromagnetism where penetrable non-magnetic materials have magnetic permeability $\mu = 1/B = 1$ and large permittivity $|\epsilon|$ [14–16] (typically a metal approaching perfect conducting condition), which makes $1/k_1$ to vanish. In acoustics, this limit is less problematic, since materials have relatively small variability in sound velocity (usual sound velocities differ typically by a factor of 10) and the variation of impedance is attributable to the variation in the mass density (typical variations can be on the order of 10^3). Thus, it is possible to conceive sound-soft materials with finite values of ρ_1/B_1 and thus of $1/k_1$. Therefore, one possible way to move from sound-hard to sound-soft materials, and the one that we consider in the following, is along a trajectory with finite (constant) α and varying q from the limit of sound-hard material ($q \to 0$) to the limit of sound-soft materials ($q \to \infty$).

Resonant guided waves, as spoof plasmons, are the resonant modes that propagate along the y-direction while being evanescent in the x-direction. Thus, to exhibit these modes, an evanescent wave is sent from $x < 0$ with total wavenumber k and a component k_y of the wavenumber along y, with $k_y > k$. In the homogenized problem, k_y is conserved in $x \geq 0$ and the wavefield can be written as

$$\begin{cases} p(x<0) = e^{ik_y y} \left[e^{i\sqrt{k^2-k_y^2}x} + Re^{-i\sqrt{k^2-k_y^2}x} \right], \\ p(0 \leq x < \ell) = e^{ik_y y} \left[Ae^{ik_{\text{e}}x} + Be^{-ik_{\text{e}}x} \right], \\ p(x \geq \ell) = Te^{i(k_y y + \sqrt{k^2-k_y^2}x)}, \end{cases} \tag{5}$$

with $k_{\text{e}} = \sqrt{(B_0/B)(\rho_x/\rho_0)k^2 - (\rho_x/\rho_y)k_y^2}$, the component of the wavenumber along x in the birefringent guide, with the convention that $e^{ik_{\text{e}}x}$ refers to a wave propagating along $+x$. The problem is easy to solve and guided waves are found by means of divergences in the reflection and transmission coefficients, R and T, respectively. We report the expression of R,

$$R = \frac{\xi^2 - 1}{(\xi - i \tan k_{\text{e}}\ell/2)(\xi + i/\tan k_{\text{e}}\ell/2)}, \tag{6}$$

where $\xi \equiv \frac{\rho_x \sqrt{k^2-k_y^2}}{\rho_0 k_{\text{e}}}$ is the ratio of the impedances between the external medium and the birefringent material. Resonant guided waves follow two branches and we report the dispersion relation of the first branch

$$\xi = i \tan k_{\text{e}}\ell/2 \tag{7}$$

which is obtained for $k_y = k_{\text{SP}}$.

At this stage, we can remark that the waves guided in the birefringent slab have to be propagating. Indeed, if it is not the case, k_{e} is imaginary, and thus the right hand side term in Eq. (7) is real negative, while ξ is real positive. Thus, resonant guided waves propagate in the birefringent medium with wavenumber k_{e} along x, and with wavenumber k_{SP} along y, and are evanescent in the surrounding medium.

Using the expressions for the effective parameters, Eqs. (4), the dispersion relation can be written in terms of the parameters (α, q) (and the filling fraction φ)

$$\begin{cases} \xi = f(\alpha, q) \sqrt{\dfrac{k^2 - k_y^2}{n_{\text{e}}^2 k^2 - k_y^2}}, \\ k_{\text{e}} = g(\alpha, q) \sqrt{n_{\text{e}}^2 k^2 - k_y^2}, \end{cases} \tag{8}$$

with n_{e} the refractive index along x,

$$n_{\text{e}} \equiv \sqrt{(\varphi\alpha q + 1 - \varphi)\left(\frac{\varphi\alpha}{q} + 1 - \varphi\right)}, \tag{9}$$

and

$$\begin{cases} f(\alpha, q) \equiv \left(\dfrac{\varphi q}{\alpha} + 1 - \varphi\right)^{-1/2} \left(\dfrac{\varphi\alpha}{q} + 1 - \varphi\right)^{1/2}, \\ g(\alpha, q) \equiv \left[\left(\dfrac{\varphi q}{\alpha} + 1 - \varphi\right)\left(\dfrac{\varphi\alpha}{q} + 1 - \varphi\right)\right]^{-1/2}. \end{cases} \tag{10}$$

It is our goal to describe the guided waves in our homogenized problem for q going from zero to infinity. Thus, one has to choose α to ensure the existence of solution, which is satisfied if $\alpha \geq 1$. In the limiting case $q \to 0$ of sound-hard inclusions (with $k_e \to k$ and $\xi \to i\sqrt{k_y^2/k^2 - 1}/(1-\varphi)$ in Eq. (7)),

$$k_{SP} = k\left[1 + (1-\varphi)^2 \tan^2 k\ell/2\right], \qquad (11)$$

we recover the usual dispersion relation [2, 3], since the array is equivalent to a grating by symmetry. In the limit $q \to \infty$ of sound-soft inclusions, the dispersion relation becomes

$$k_{SP} \simeq \left[\sqrt{\varphi(1-\varphi)}\sqrt{\frac{B_0}{B_1}} - \frac{1-\varphi}{k\ell}\right] k. \qquad (12)$$

Note that the dominant term, corresponding to $k_{SP} \simeq n_e k$ with $n_e \propto \sqrt{B_0/B_1}$, is close to the light line, or sound line, of the birefringent waveguide. Thus, k_{SP}/k can reach very high values, well beyond the relative refractive index $\alpha = c_0/c_1$ of the inclusions. Therefore, a structured array of inclusions can support spoof plasmons with wavelength much smaller than a simple layer of the same material. Below, we confirm our prediction by comparing the homogenized problem with direct numerical calculations [17].

We consider the configuration of Fig. 1(a) with $\ell = 3d$, $\varphi = 0.7$, and $\alpha = 1.25$. In order to satisfy the large wavelength approximation within the first Brillouin zone, we vary kd and $k_y d$ between zero and $\pi/2$. The reflection coefficient $|R^{ex}|$ as a function of k and k_y is reported in Fig. 2 (upper panel) and compared with the reflection coefficient R in the homogenized problem of Fig. 1(b), Eq. (6), (lower panel), for $q = 10^{-6}$, 10^{-1} 10 and 10^2. The agreement is excellent in all cases.

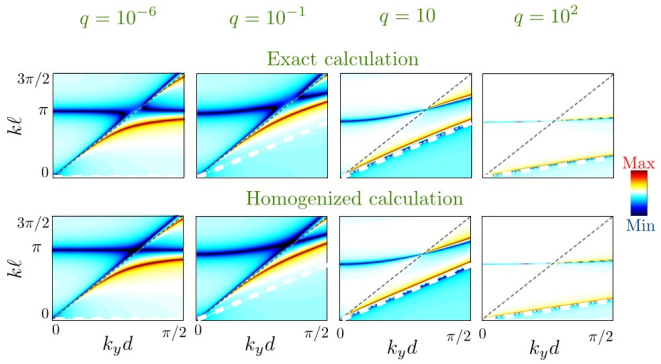

FIG. 2: Reflection coefficient in the (k_y, k) space for different impedance ratios q (color scale is in log scale). The upper panels show $|R^{ex}|$ in the exact calculations, Fig. 1(a), and the lower panels show $|R|$, Eq. (6), in the homogenized calculation, Fig. 1(b). The black dashed line represents the sound line of the air, $k = k_y$. The white dashed line corresponds to the sound line of the birefringent waveguide, $n_e k = k_y$.

In Figs. 2(a) and (b), the dispersion relation of the spoof plasmon in the array is visible by means of diverging $|R^{ex}|$ and $|R|$, respectively (red zones). As expected, the spoof plasmons take place in the regions of the (k_y, k)-space below the sound line of the air ($k < k_y$) and above the sound line of the birefringent layer ($n_e k > k_y$). In the homogenized problem, n_e is close to infinity for $q \to 0$ and the corresponding sound line is reduced to $k = 0$ (the wave is always propagating in the slab with wavenumber k along x). Increasing q toward unity first produces a slope increase of the sound line $n_e k = k_y$ (with maximum value being $(\varphi\alpha + 1 - \varphi)$, leading to a transparent effective medium if $\alpha = 1$). Nevertheless, the plasmon wavenumber remains almost unchanged during this first phase, with $k_{SP}/k \leq \ell/d$. Increasing further q produces a slope decrease of the sound line of the slab. But here, the spoof plasmon follows the sound line of the birefringent waveguide, resulting in an increase of k_{SP}/k.

This scenario is further illustrated in Fig. 3, which shows the behavior of $|R^{ex}|$ as a function of k and q, for fixed $k_y d = 1$. The transition is visible between $q < 1$ where the plasmon (red peak $k = k_{SP}$) remains stuck to the sound line of the air $k = k_y$, and $q > 1$ where the plasmon wavenumber k_{SP} follows the sound line of the birefringent slab ($k_y = n_e k$). It is important to note that this latter sound line has no physical meaning in the real problem. The dashed white line shows the dispersion relation for the guided waves in the homogenized problem, Eq. (7). As previously observed, the agreement is excellent between the exact calculation and the analytical dispersion relation of the trapped waves in the homogenized problem. Notably, the scaling law predicted in Eq. (12) is confirmed, with the plasmon wavenumber scaling as $k_{SP}/k \propto \sqrt{q}$.

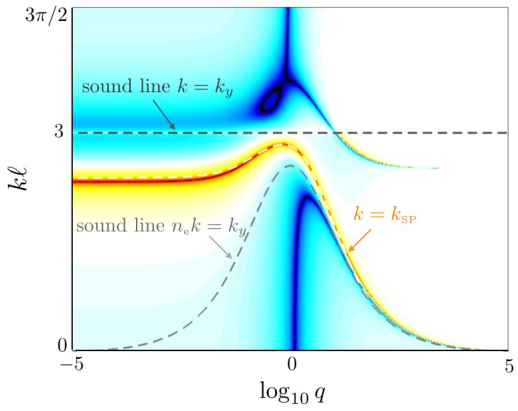

FIG. 3: Dispersion relation as a function of the impedance ratio q for $k_y d = 1$, evidenced by the divergence of $|R^{ex}|$ in the array of inclusions (red zones). The dispersion relation of the guided wave in the homogenized problem $k = k_{SP}$, Eq. (7), is indicated in white dotted line.

We have said that sound soft materials for waves are now available and we end with an example of possible experiments. An excellent candidate for sound soft material is air in water (Fig. 4), for which $q = \rho_{water} c_{water}/\rho_{air} c_{air} \simeq 4.10^3$ and $\alpha = c_{water}/c_{air} \simeq 4$. Polydimethylsiloxane

(PDMS), which has similar acoustical properties than water, provides a way to encapsulate air [18–20]. We numerically consider two configurations: an array of rectangular inclusions of air (encapsulated in PDMS, Fig. 4(b)), and for comparison, a layer of air encapsulated in PDMS (Fig. 4(a)). Realistic dimensions are $d = 0.5$ mm with $\ell = 0.1d$ or $\ell = d$; for the array, we use $\varphi = 0.8$ and $\varphi = 0.9$ (the waveguide corresponds to $\varphi = 1$), for frequencies $f = 20$ kHz ($\lambda = 7$ cm in water). This allows to avoid Mie resonances [21] and Minnaert resonances [18–20] and thus, only the contrast in the materials is concerned.

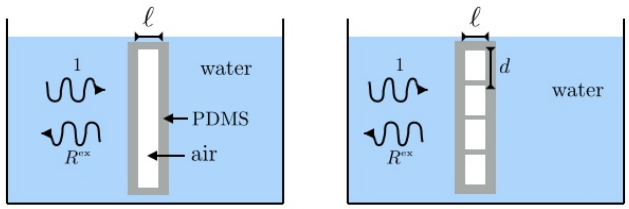

(a) (b)

FIG. 4: Example of possible set-up. (a) Guided waves by a layer of air in water ($\varphi = 1$). (b) Spoof plasmon in a structured array of air inclusions in water. In practice, air can be encapsulated in PDMS; $d = 0.5$ mm and $\ell = 0.1d$ or $\ell = d$.

Figure 5 reports the variation of the reflection coefficient $|R^{ex}|$ as a function of k_y. When the layer of air is used, the spoof plasmon simply corresponds to a wave guided within the layer of air being given by $k_{SP} \simeq \alpha k \simeq 4k$. For the arrays of air inclusions, λ_{SP} is tuned by changing the filling fraction φ and the width of the array ℓ, in agreement with our homogenized prediction, Eq. (12). Figure 6 shows the sub-wavelength plasmon fields realizing $\lambda_{SP} \sim \lambda/20$, $\lambda/40$, and $\lambda/60$. It is worth noting that realizing such subwalength plasmons using metallic wires would require much larger dimensions of the structures. This is because, one has to use ℓ being scaled by the working frequency $k\ell \sim \pi$ to get large relative $k_{SP}/k \simeq \ell/d$ (Eq. (11)). In the presented cases, this would require $\ell = 35$ mm and $d = 1.75$ mm (SP_1), $d = 0.87$ mm (SP_2) and $d = 0.5$ mm (SP_3).

In summary, we have reported a new way to design ultra compact arrays supporting sub-wavelength plasmons (in the presented examples, $k\ell \sim 10^{-2} - 10^{-3}$, leading to plasmons with tunable wavelength up to $\lambda/100$). Such arrays have promising applications in imaging and wave propagation control at deep sub-wavelength scale in water, and can be built using microfluidic techniques to encapsulate air cavities in polymer materials. Besides, the plasmon excitation does not find its origin in cavity resonances, resulting in a broadband validity of the dispersion relation. Finally, tunable acoustic metamaterials based on such soft inclusions are possible owing to the proven sensitivity of cavities in gel matrix to external shears or to external magnetic and electric fields.

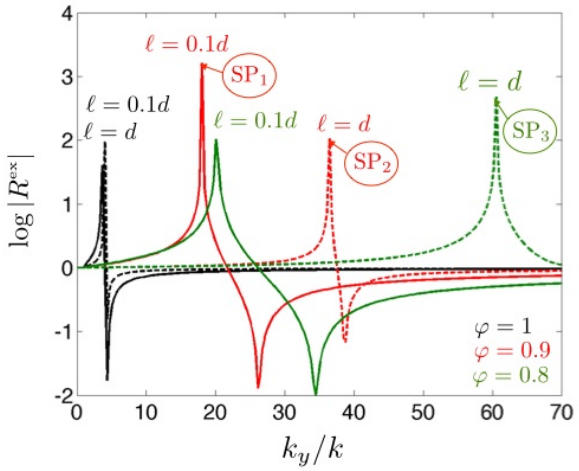

FIG. 5: Exact reflection coefficient $|R^{ex}|$ as a function of λ/λ_{SP} at $f = 20$ kHz ($\lambda = 7$ cm for $d = 0.5$ mm) for $\ell = 0.1d$ (solid lines) and $\ell = d$ (dashed lines). The black lines show the results for an air waveguide (Fig. 4(a), $\varphi = 1$): $\lambda_{SP} \simeq \lambda/4$. Red and green lines show the results for a structured array of rectangular air inclusions in PDMS (Fig. 4(b)): for $\varphi = 0.9$, $\lambda_{SP} \simeq \lambda/20, \lambda/40$ and for $\varphi = 0.8$, $\lambda_{SP} \simeq \lambda/20, \lambda/60$.

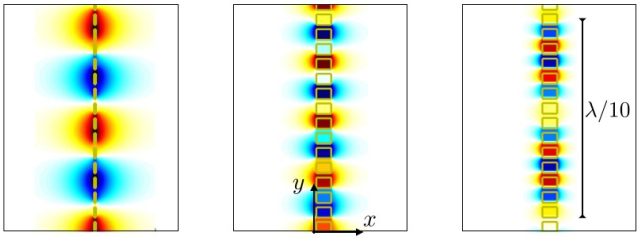

(a) SP_1 (b) SP_2 (c) SP_3

FIG. 6: Wavefield of the sub-wavelength plasmons in the array of Fig. 4(b), for frequency $f = 20$ kHz ($\lambda = 7$cm). (a-c) refer to the $SP_{1,2,3}$ in Fig. 5.

Acknowledgments

This work has been initiated during the ANR- Conicyt PROCOMEDIA project. The authors acknowledge the support of the french Agence Nationale de la Recherche and to the chilean Conicyt.

[1] J. B. Pendry, L. Martín-Moreno, F.J. Garcia-Vidal, Science. **305** 5685 (2004) 847-848.

[2] F.J. Garcia-Vidal, L. Martín-Moreno, J. B. Pendry, J. Opt. A: Pure Appl. Opt. **7** (2005) S97-S101.

[3] L. Kelders, J.F. Allard, W. Lauriks, J. Acoust. Soc. Am. **103**(5) (1998) 2730-2733.
[4] J. Zhu, Y. Chen, X. Zhu, F.J. Garcia-Vidal, X. Yin, W. Zhang, X. Zhang, Scientific Rep. **3** 1728 (2013).
[5] K. Song, S-H. Lee, K. Kim, S. Hur, J. Kim, Scientific Rep. **4** 4165 (2014).
[6] I. Thompson and C. M. Linton, SIAM J. Appl. Math. **70**, 2975-2995 (2010).
[7] F. Lemoult, N. Kaina, M. Fink and G. Lerosey, Nature Phys. **9** 55 (2013)
[8] M. Kadic, T. Bückmann, R. Schittny, P. Gumbsch, and M. Wegener, Pentamode Metamaterials with Independently Tailored Bulk Modulus and Mass Density Phys. Rev. Appl. **2** 054007 (2014).
[9] A Cebrecos, V Romero-García, R Picó, V J Sánchez-Morcillo, M Botey, R Herrero, Y C Cheng and K Staliunas, J. Phys. D: Appl. Phys. **48** 025501 (2014).
[10] N. Aközbek, N. Mattiucci, M. J. Bloemer, M. Sanghadasa, and G. D'Aguanno, Appl. Phys. Lett. **104** 161906 (2014).
[11] X. Zheng, H. Lee, T. H. Weisgraber, M. Shusteff, J. DeOtte, E. B. Duoss, J. D. Kuntz, M. M. Biener, Q. Ge, J. A. Jackson, S. O. Kucheyev, N. X. Fang, and Ch. M. Spadaccini, Science **344**, 1373 (2014).
[12] A. Maurel, S. Félix and J.F. Mercier, Phys. Rev. B **88**, 115416 (2013).
[13] J. Christensen, Z. Liang, M. Willatzen, Phys. Rev. B **88** (2013) 100301(R).
[14] N.A. Nicorovici, R.C. McPhedran and L.C. Botten Phys. Rev. Lett. **75**(8), 1507 (1995).
[15] A.B. Movchan, C.G. Poulton, L.C. Botten, N.A. Nicorovici, and R.C. McPhedran, SIAM Journal on Applied Math., **61**(5) 1706-1730 (2001).
[16] D. Felbacq, J. Math. Phys. **43** 52 (2002).
[17] We use a modal method already presented in : A Maurel, J.-F. Mercier and S. Félix, J. Acoust. Soc. Am. **135**(1) 165-174 (2014).
[18] V. Leroy, A. Bretagne, M. Fink, H. Willaime, P. Tabeling and A. Tourin, Appl. Phys. Lett. **95** 171904 (2009).
[19] V. Leroy, A. Strybulevych, J.H. Page, and M.G. Scanlon, Phys. Rev. E **83**(4) 046605 (2011).
[20] E. L. Thomas, Nature **462**(7276), 990-991 (2009).
[21] T. Brunet, J. Leng and O. Mondain-Monval, Science **342**(6156), 323-324 (2013).